Available online at www.sciencedirect.com
ScienceDirect
Journal of Power Sources 168 (2007) 12–21
JOURNAL OF POWER SOURCES
www.elsevier.com/locate/jpowsour

Advanced valve-regulated lead-acid batteries for hybrid vehicle applications

M.L. Soria *, F. Trinidad, J.M. Lacadena, A. Sánchez, J. Valenciano

Exide Technologies, Research & Development Centre, Autovía A-2, km 42, E-19200 Azuqueca de Henares, Spain

Received 22 September 2006; received in revised form 21 November 2006; accepted 21 November 2006
Available online 16 January 2007

Abstract

Future vehicle applications require the development of reliable and long life batteries operating under high-rate partial-state-of-charge (HRPSoC) working conditions. Work presented in this paper deals with the study of different design parameters, manufacturing process and charging conditions of spiral wound valve-regulated lead-acid (VRLA) batteries, in order to improve their reliability and cycle life for hybrid vehicle applications.

Test results show that both electrolyte saturation and charge conditions have a strong effect on cycle life at HRPSoC performance, presumably because water loss finally accelerates battery failure, which is linked to irreversible sulphation in the upper part of the negative electrodes. By adding expanded graphite to the negative active mass formulation, increasing the electrolyte saturation degree (>95%) and controlling overcharge during regenerative braking periods (voltage limitation and occasional boosting) it is possible to achieve up to 220,000 cycles at 2.5% DOD, equivalent to 5500 capacity throughput.

These results could make lead acid batteries a strong competitor for HEV applications versus other advanced systems such as Ni–MH or Li-ion batteries.

Keywords: Valve-regulated lead-acid batteries; Spiral wound; Cycle life; Charging strategies; Hybrid vehicles

1. Introduction

Environmental concerns and already established terms to reduce vehicle emissions support the development of mild hybrid vehicles in Europe, with functions such as stop-start, boosting and regenerative braking. Efficient energy management in vehicles with such functions demands the development of batteries with improved charge acceptance as well as longer life under high-rate partial-state-of-charge (HRPSoC) working conditions [1].

Previous work on the development of spiral wound valve-regulated lead-acid (VRLA) batteries for future automotive applications was focused on active material formulations to improve cycle life under high rate partial state of charge working conditions, and demonstrated the high power capability of this battery design as well as the life increase achieved by means of the addition of expanded graphite to the negative active material formulation [2,3].

Within the ALABC ISOLAB project [4], different battery design and process parameters have been studied, in order to improve the reliability and cycle life of spiral wound VRLA batteries for HEV applications. Although irreversible sulphation of the upper part of the negative electrodes has been previously considered as the main battery failure mode under HRPSoC conditions [5], water loss and local heating could also promote and accelerate such ageing mechanisms and therefore, valve opening pressure, initial electrolyte saturation degree as well as charging conditions along the life test have been considered as key parameters to improve cycle life of VRLA batteries.

A higher valve opening pressure may allow the development of higher internal pressure inside the battery and thus a higher gas accumulation reducing the water loss in the cells.

Although for deep cycling applications a lower saturation degree favours complete and consistent IUi charging and, thus, balances the charge completion of positive and negative plates, floating and shallow cycle applications may respond to different

* Corresponding author. Tel.: +34 949 263 316; fax: +34 949 262 560.
E-mail addresses: MariaLuisa.SORIA@eu.exide.com (M.L. Soria), Francisco.TRINIDAD@eu.exide.com (F. Trinidad), JoseManuel.LACADENA@eu.exide.com (J.M. Lacadena), Jesus.VALENCIANO@eu.exide.com (J. Valenciano).

0378-7753/$ – see front matter © 2006 Elsevier B.V. All rights reserved.
doi:10.1016/j.jpowsour.2006.11.086

working conditions. In mild hybrid partial state of charge operation, battery complete recharging is infrequent. Provided that performance is not reduced by electrolyte saturation, a higher saturation degree may suppress any occasional negative active material oxidation and the increased electrolyte reserve may be beneficial for applications at higher temperatures and with difficult charge control.

Finally, the use of different charging conditions, with occasional boosting phases, would allow to establish the best compromise between recuperation of braking energy (favoured by higher charging voltages) and life limitation due to battery overcharge or undercharge.

2. Experimental

2.1. Battery assembly

The 6 V/24 Ah spiral wound module prototypes, sized 175 mm × 65 mm × 190 mm, were assembled with coils prepared winding positive and negative plates and absorptive glass mat (AGM) separator materials. They presented several design improvements, compared to previous modules [2], that ensured isolation of individual cells as well as a larger acid reservoir to improve the battery filling and formation processes. Positive and negative electrodes were prepared pasting lead-tin alloy concast grids with specific active material formulations adapted to high power and partial state-of-charge battery working conditions, and described previously [3].

To establish the influence on battery life of the design and process parameters considered in this study, different batches of modules have been assembled, according to the characteristics mentioned in Table 1. It shows the experimental matrix with the range of values of the controlled variables in each batch.

To study the effect of the valve opening pressure, prototypes were assembled using valves manufactured with different rubber materials. Bunsen valves prepared with rubber materials with 50°, 60° and 70° Shore A nominal hardness, led to opening pressure values of 20, 45 and 100 kPa, respectively, on preliminary calibration measurements.

The effect of the electrolyte saturation degree was studied controlling the filling acid quantities so that, after battery formation, the saturation degree was estimated as 90, 95 and 100%.

Results from the valve opening pressure and saturation degree studies were used to select the characteristics of the prototypes for the charging conditions study, which included charging voltages of 2.4, 2.5 and 2.66 V cell^{-1} and occasional boosting periods every 500 cycles of 2 h at 2.5 V cell^{-1}.

2.2. Electrical testing

Electrical testing of the batteries was carried out with computer controlled cycling equipment: Bitrode LCN-7-100-12 for initial characterisation and cycle life tests of 6 V modules, Digatron UBT BTS-500 mod. HEW 2000-6BTS in high rate discharges and Digatron HEW 2000/12-700/36 BTS-600 for characterisation and cycling of a 36 V battery.

Preliminary characterisation of the modules included C_{20} capacity (1.2 A, 25 °C) and cold cranking at 400 A and −18 °C. Cycle life test was carried out according to EUCAR power assist profile, at 60% SOC, 2.5% DOD and 5 C discharge rate [6], which simulates vehicle boost during acceleration and recovery of braking energy. During the test, the modules were air draught cooled by means of fans located under the modules. Every 10,000 cycles the C_2 capacity (10.0 A, 25 °C), AC internal resistance (measured with a Milliohmeter Hewlett Packard mod. 4338-B at 1 kHz and 25 °C) and weight loss of the modules were checked.

When the modules reached the failure criterion ($V < 1.5$ V cell^{-1}), they were recharged and torn down to determine the failure mode. Chemical analyses of the active material samples were carried out using internal volumetric (PbO_2) and gravimetric ($PbSO_4$) procedures. Active material porosity was measured with a mercury intrusion porosimeter Micromeritics Autopore 9405 and specific surface (BET) with a Micromeritics FlowSorb II 2300. Finally, the morphological studies have been carried out with the Scanning Electron Microscope Hitachi S-3000N, model INCAx-sight.

To check the reliability and durability of the different valve materials (with opening pressures of 20, 45 and 100 kPa), three modules of each type were connected in series and tested at constant voltage overcharge conditions, at a floating voltage of 20.4 V, equivalent to 2.27 V cell^{-1}, in a heated chamber at 55 °C to accelerate ageing processes, as described in the British Standard BS 6290 (Part 4). These conditions can also simulate

Table 1
Experimental matrix with design and process conditions

Reference	Valve opening pressure (kPa)	Electrolyte saturation (%)	Charge voltage maximum (V cell^{-1})	Boost (every 500 cycles)
20 kPa	20	97	2.66	No
45 kPa	45	97	2.66	No
100 kPa	100	97	2.66	No
90%	20	90	2.66	No
95%	20	95	2.66	No
100%	20	100	2.66	No
2.66 V cell^{-1}	20	97	2.66	No
2.5 V cell^{-1}	20	97	2.5	No
2.5 V cell^{-1} + boost	20	97	2.5	2 h at 2.5 V cell^{-1}
2.4 V cell^{-1} + boost	20	97	2.4	2 h at 2.5 V cell^{-1}

battery use during vehicle operation (1000 h, or rather 42 days, use per year, at the temperature of the engine compartment). After each 42 day life unit, the batteries were discharged at room temperature to check the available capacity at the 2 h rate (10.0 A until 1.75 V cell^{-1}), AC internal resistance and weight loss, and then placed again in the heated chamber at the floating voltage.

2.3. Thermal study of a 36 V system

The thermal study of a 36 V battery has been carried out to determine the influence of air draught cooling and charging voltage on the temperature at different module positions in a 36 V system for hybrid electric vehicle applications, as well as the ageing effects of working temperature on the modules. The battery was assembled with six modules similar to those used for the charge conditions study, which were connected in series.

The 36 V system was submitted to a partial-state-of-charge cycling test (Power Assist Cycle Life Test according EUCAR procedure) at 2.5% DOD and 60% SOC. The temperature evolution is very important in this HRPSoC cycling test because the selective accumulation of lead sulphate in negative plates of spiral configuration depends on it. The aim of this test was to check the effect of different air draught cooling rates and constant charge voltages on the temperature evolution in different locations of the battery. To refrigerate the 36 V system, three fans (ebm W2G115-AD19-02, 48 V DC, 4.6 W) were located in the bottom of the 36 V battery.

For the temperature recording, thermocouples were fixed to six different positions of the battery, as shown in Fig. 1: on one external side of module 6, on module 2 between modules 2 and 3 and on module 3 between modules 3 and 4. Data were recorded automatically with a data logger connected to a portable computer. Finally, Table 2 shows the detailed test profile with power assist cycling at three different charging voltage conditions (43.2, 45.0 and 48.0 V) and two cooling rates (high level of 2667 l min^{-1} and low level of 1333 l min^{-1}, with external voltage inputs of 40.0 and 20.0 V, respectively). A sequence of 700 microcycles was carried out at each charging voltage and cooling rate and rest periods of 90 min were programmed between the 700 cycle sequences, to let the battery cool down. After the six sets of 700 cycles, 5800 power assist cycles were carried out

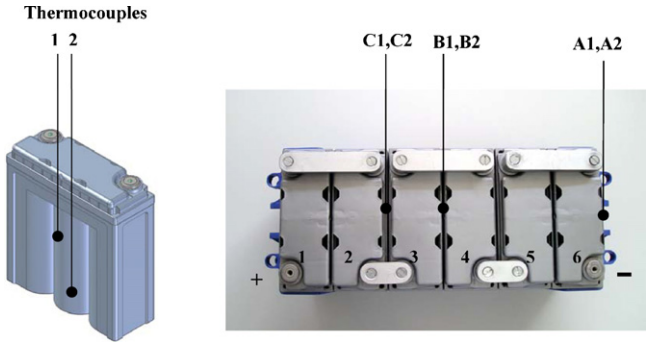

Fig. 1. Six volt module, 36 V battery and location of thermocouples for the thermal study.

Table 2
Testing conditions of the thermal study

	Test conditions	Air cooling rate (l min^{-1})
Discharge 60% SOC	10 A, 48 min	2667
700 PA cycles[a]	Charge 43.2 V	
700 PA cycles[a]	Charge 45 V	
700 PA cycles[a]	Charge 48 V	
700 PA cycles[a]	Charge 43.2 V	1333
700 PA cycles[a]	Charge 45 V	
700 PA cycles[a]	Charge 48 V	
5800 PA cycles[a]	Charge 45 V	
Charge	43.2 V/6 A/6 h + 0.6 A/4 h	
Rest	2 h	
2 h capacity check	10 A	
Charge	43.2 V/6 A/20 h + 0.6 A/4 h	

[a] PA: power assist cycle; 90 min rest after each 700 PA sequence.

to complete the 10,000 microcycle life unit, charging at 45.0 V and at the lower cooling rate (1333 l min^{-1}). A capacity check and a full charge were performed before starting a new life unit.

3. Results and discussion

3.1. Initial characterisation of 6 V modules

Table 3 shows the results of the preliminary characterisation of the modules. In the initial tests, no significant differences,

Table 3
Initial electrical test results of 6 V modules with different design and process parameters

Reference	Weight (kg)	Resistance (mΩ)	C_{20} capacity (Ah)	Cold cranking (400 A)	
				Voltage (10 s) (V)	Time (3.6 V) (s)
20 kPa	4.72	2.36	24.1	3.87	27
45 kPa	4.71	2.37	24.1	3.82	26
100 kPa	4.71	2.34	24.0	3.84	25
90%	4.67	2.28	24.2	3.90	23
95%	4.71	2.24	24.3	4.00	27
100%	4.74	2.21	24.3	4.03	26
2.66 V cell^{-1}	4.72	2.36	24.1	3.87	27
2.5 V cell^{-1}	4.81	2.38	24.7	3.88	29
2.5 V cell^{-1} + boost	4.74	2.44	24.5	3.78	25
2.4 V cell^{-1} + boost	4.80	2.38	24.7	3.78	24

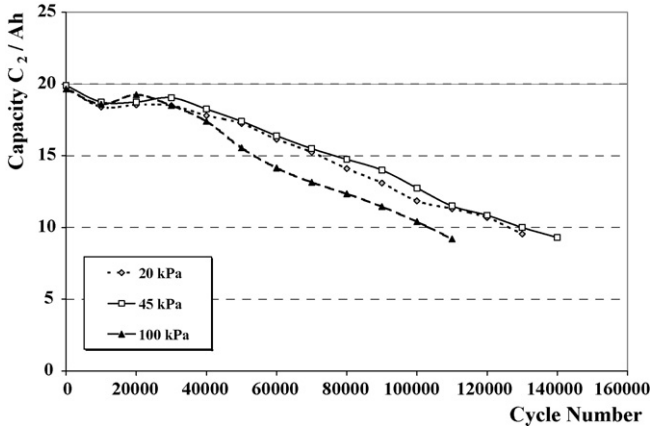

Fig. 2. Capacity evolution of modules with different valve opening pressures along the power assist cycle life test.

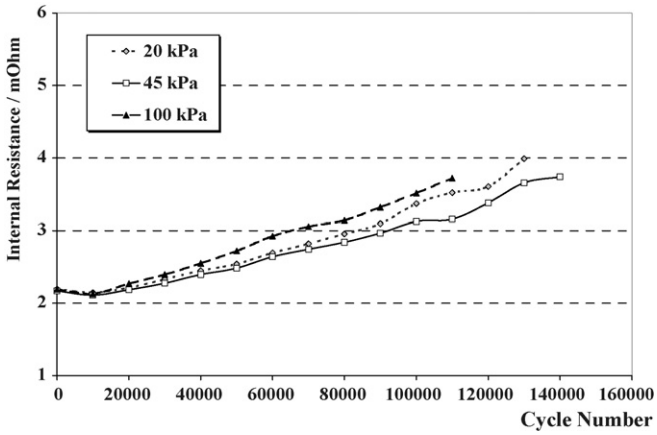

Fig. 3. Internal resistance of modules with different valve opening pressures along the power assist cycle life test.

that could be related to the design changes, have been observed among the different groups.

3.2. Life tests of modules with different valve opening pressure

Fig. 2 shows the capacity evolution during the power assist life test of the modules having different valve opening pressures. The capacity difference observed along the life test between the modules with 20 and 45 kPa valve opening pressures is not considered significant for the application. However modules with high pressure valves (100 kPa) showed a higher capacity decay, and the reason for that behaviour was determined in the tear down at the end of life test, as it was confirmed that high working pressure stressing of the lid/container welding had resulted in some small leakages, thus accelerating water loss.

In order to estimate the power capability evolution of the modules along cycle life test, the impedance at 1 kHz (AC resistance) has been also determined after the capacity control every 10,000 cycles. The behaviour is quite similar for the three types of modules and relatively independent of the valve opening pressure. However, data indicate that in the modules with the highest valve pressure (100 kPa) the internal resistance increases at a faster rate than in the other groups. As shown in Fig. 3, the lowest internal resistance values along life correspond to modules with 45 kPa valve opening pressure.

Weight loss has also been measured during the life test and figures obtained at battery failure represent around 5 wt.% of the initial electrolyte weight for modules with valve opening pressure of 20 and 45 kPa. As shown in Fig. 4, the lowest accumulated weight loss values correspond to modules with 45 kPa as valve opening pressure, which may better retain the gases under high rate PSOC conditions. In the modules with the highest opening pressure (100 kPa), after 40,000 cycles, the weight loss increased at a faster rate. The reason for this behaviour is the development of small leakages in the lid/container thermowelding that could not withstand such high internal pressure. The increased weight loss is probably the main reason for the more pronounced capacity decay after 40,000 cycles shown in Fig. 2.

Weight loss has been mainly ascribed in all the tests performed to gas evolution and water vapour loss, promoted by high temperature battery operation. Ohmae et al. have recently reported on the relationship between temperature and water consumption in VRLA batteries for advanced vehicle applications, due to increased gas evolution on overcharge and water loss from evaporation at battery temperatures over 60 °C [7].

Fig. 5 shows the capacity evolution of the modules having different valve opening pressures (20, 45 and 100 kPa) measured after each 42 days life unit of the overcharge test at 2.27 V cell^{-1} and 55 °C. There are no clear differences in available capacity among the three types, that was practically constant until the sixth unit, and then it dropped dramatically. The modules completed the six units with capacity values similar or higher than the initial 2-h rated capacity (20 Ah). According to Arrhenius law, every 10 °C temperature increase, ageing phenomena rates are doubled, and thus, performing the tests at 55 °C accelerates the processes 11.3 times, with respect to 20 °C. That means that every 42-days life unit corresponds to 1.3 years floating overcharge at an average of 20 °C and this result corresponds to about 8 years of floating life at 20 °C, a very good durability result for high rate VRLA batteries with thin plate design.

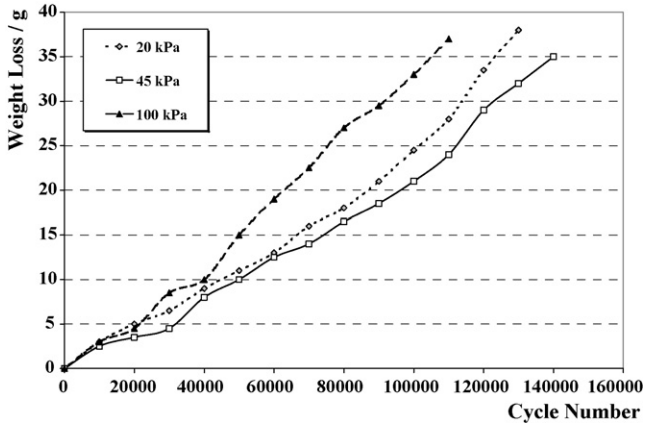

Fig. 4. Accumulated weight loss of modules with different valve opening pressures along the power assist cycle life test.

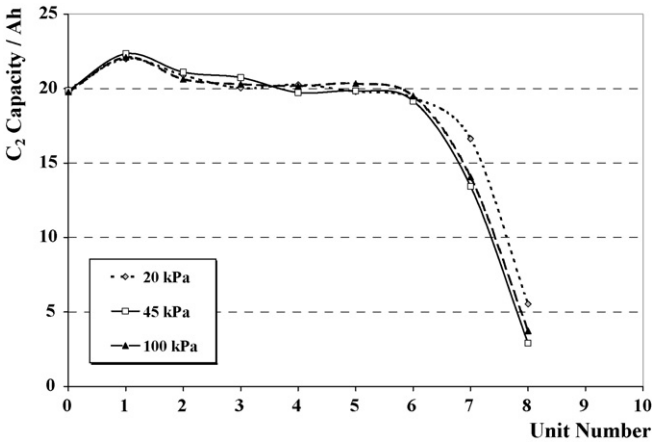

Fig. 5. Capacity evolution of modules with different valve opening pressures along floating test at 2.27 V cell^{-1} and 55 °C.

The significant capacity loss observed after the 6th life unit has been ascribed to the increase of internal resistance. Fig. 6 shows the impedance values of the modules at 1 kHz measured after each life unit was completed. The values obtained with the three valve types are very similar and relatively independent of the valve opening pressure and reveal that, after the fifth life unit, the internal resistance increased exponentially, reaching values up to 35–45 mOhm (15–20 times the initial values) at battery failure.

Battery weight was also checked after each overcharge life unit to establish if there was any relationship with the valve opening pressure. Fig. 7 shows the accumulated weight loss along the overcharge test and no significant differences between prototypes can be appreciated. The average weight loss is about 10 g per life unit and represents at the end of life 10 wt.% of the initial electrolyte weight. It was expected that modules with higher vent opening pressure (100 kPa) should last longer than the others, however, they showed in fact similar behaviour to modules with lower opening pressures. This experimental fact could only be explained if water loss is not the main failure mode under floating conditions, as already shown by the weight

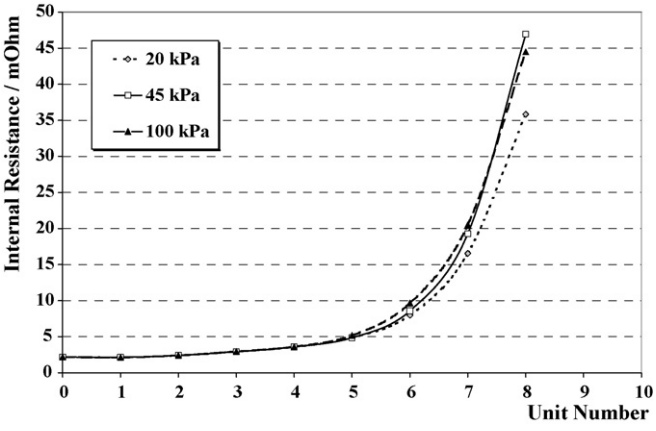

Fig. 6. Internal resistance of modules with different valve opening pressures along the floating test at 2.27 V cell^{-1} and 55 °C.

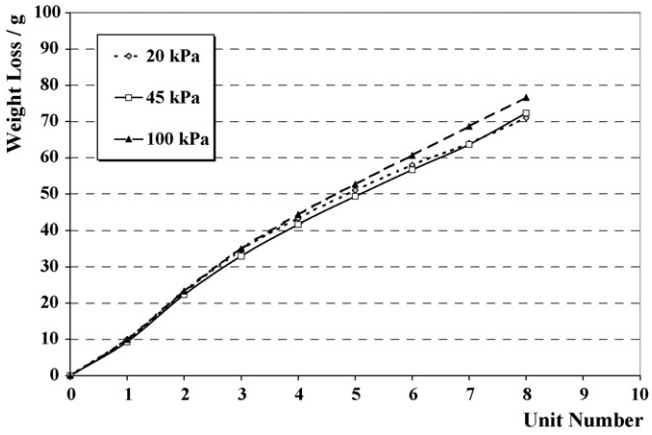

Fig. 7. Accumulated weight loss of modules with different valve opening pressures along the floating test at 2.27 V cell^{-1} and 55 °C.

loss measurements, with no significant differences among the different valve opening pressures.

Finally, tear-down analysis of the batteries after failure showed strong corrosion of positive grids, as expected due to the ageing conditions, that provoked a significant conductivity loss in the plates and the subsequent exponential internal resistance increase. Corrosion of positive grids has been reported as major failure mode in batteries subjected to extensive overcharge conditions [8], and water loss in VRLA batteries, up to a critical value often quoted as 10 wt.% of the initially available electrolyte, may also contribute to electrical resistance increase [9], as it would indicate a too low separator saturation level (estimated as 80–85% in our study). However, in this case, corrosion of positive grids is considered the major cause for the exponential electrical resistance increase, because in a parallel test reported below, modules subjected to power assist cycle life test with overcharge conditions showed at battery failure similar weight loss (11%) and a much lower internal resistance (5.7 mOhm, just 2.6 times the initial values).

3.3. Life test of modules with different saturation degrees

In this study, although the three groups had similar initial performance, cycle life behaviour led to different results: as shown in Fig. 8 the modules with 100% saturation degree completed 170,000 cycles, whereas the non-saturated modules completed 130,000 cycles.

Along the whole life test, batteries with the highest saturation degree (100%) led to higher capacity values. Moreover, influence of any electrolyte stratification on performance, at higher saturation, was not significant. This is probably due to the high charging voltage (2.66 V cell^{-1}) and relatively high internal temperature developed inside the cells during the test (around 40 °C). This result indicates that the best battery design for hybrid vehicle applications is quite different from that used in deep discharge applications, probably because water loss is strongly related to the failure mode of VRLA batteries working under HRPSoC conditions.

The evolution of the internal resistance, shown in Fig. 9, can be used as an indirect measure of the power capability. Here, the

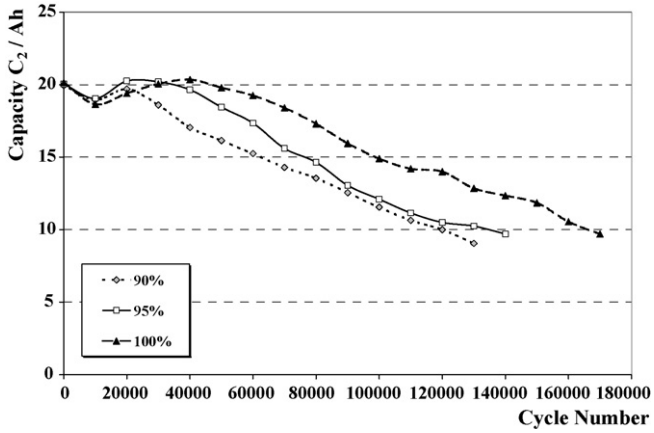

Fig. 8. Capacity evolution of modules with different saturation degrees along the power assist cycle life test.

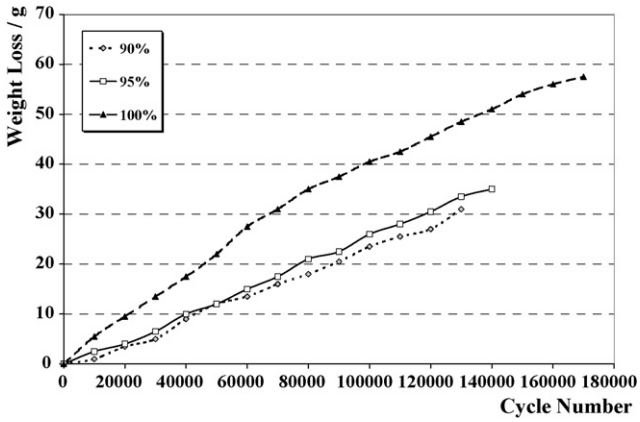

Fig. 10. Accumulated weight loss of modules with different saturation degrees along the power assist cycle life test.

initial amount of electrolyte has a significant influence on the internal resistance evolution. With low initial saturation degree (90%), the internal resistance is doubled after 130,000 cycles and therefore the instantaneous power would be reduced by half. A similar internal resistance increase was observed in saturated cells (100%) after 170,000 cycles, and this result represents over 4250 capacity turnovers.

Fig. 10 shows the accumulated weight loss along the test, which is equivalent to around 5 wt.% of the initial electrolyte weight for partially saturated modules and 8 wt.% for the 100% saturated cells, and thus directly related to the recombination rate in every case. Highly saturated cells (100%) could not effectively recombine the oxygen evolved during overcharge and thus weight loss slope is higher until cycle 60,000 when, in consequence of declining saturation, oxygen cycle rate increased and thus, weight loss slope afterwards is similar to that obtained for the modules with lower saturation degrees. However, very small differences have been observed between the partially saturated cells (90 and 95%), probably because recombination was almost equally effective in both cases and the differences in capacity and internal resistance evolution were due to the actual electrolyte remaining in the cells.

3.4. Life test of modules with different charging profiles

In order to avoid water losses due to battery overcharge, different charge strategies have been tested, with voltage limited at 2.4, 2.5 and 2.66 V cell^{-1} and including a boost charge (2 h at 2.5 V cell^{-1}) every 500 cycles to maintain an appropriate state of charge during mild hybrid HRPSoC cycling.

As shown in Fig. 11, low charge voltage limits (V = 2.4–2.5 V cell^{-1}) facilitate longer life durations (up to 220,000 cycles charging at 2.5 V cell^{-1} and 200,000 charging at 2.4 V cell^{-1} + boost), when compared to the higher charge voltage (2.66 V cell^{-1}) used in former tests. Available capacity along the power assist life test decays steadily for each level of charge voltage limit. Particularly interesting are the stable capacity values obtained at constant voltage of 2.5 V cell^{-1} charging conditions. Although an initial capacity drop was observed, probably due to partial undercharging, finally 220,000 cycles were completed. This result is close to 5500 capacity turnovers as total energy throughput. It is an impressive data never reported for VRLA batteries. High capacity values along the test were maintained with a lower voltage (2.4 V cell^{-1}) and boost period (2 h at 2.5 V cell^{-1} every 500 cycles), and the modules completed 200,000 cycles till they reached the failure criterion.

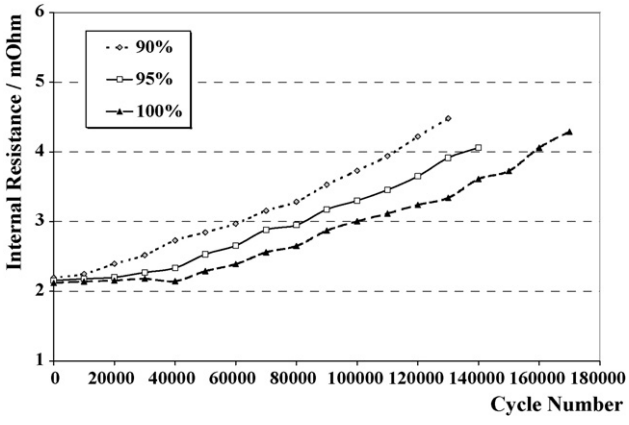

Fig. 9. Internal resistance of modules with different saturation degrees along the power assist cycle life test.

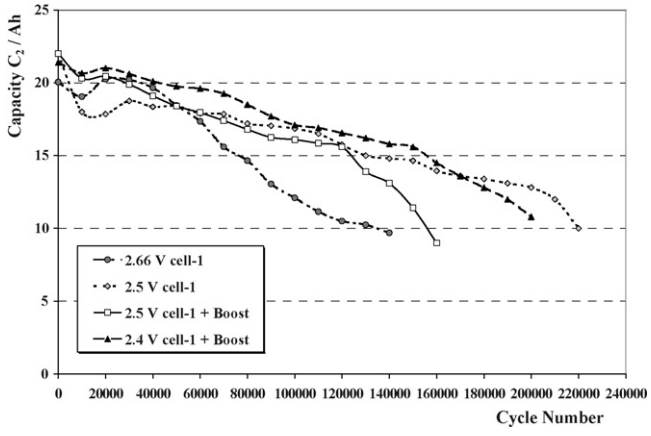

Fig. 11. Capacity evolution of modules with different charging profiles along the power assist cycle life test.

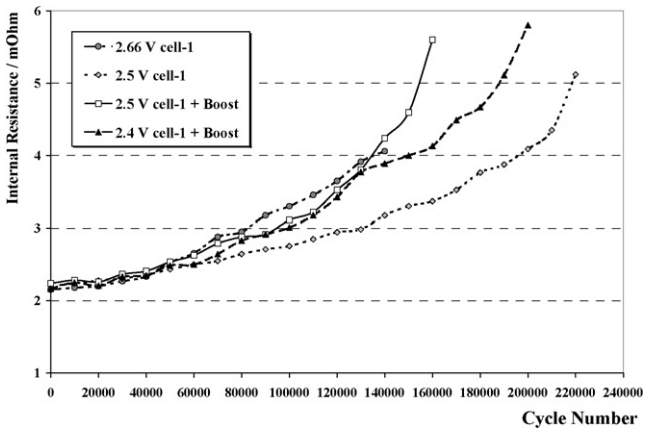

Fig. 12. Internal resistance of modules with different charging profiles along the power assist cycle life test.

These results demonstrate the need to control regenerative braking charging voltage and, moreover, that occasional boost charging could be avoided by consistent control of battery state of charge.

As shown in Fig. 12, the internal resistance evolution during the life test reflects also the benefits of controlling the overcharge by reducing the charge voltage (both at 2.4 V cell^{-1} + boost and constant voltage at 2.5 V cell^{-1}), whereas even the 'small' overcharge produced by higher voltage of 2.66 V cell^{-1} and at 2.5 V cell^{-1} with unnecessary boost tends to increase the internal resistance and reduce the available power. Results of the cycle life test indicate that boost seems to be unnecessary because internal resistance tends to increase, and capacity along life of modules charged at 2.5 V cell^{-1} is similar both with and without boost up to cycle 120,000.

Finally, Fig. 13 shows that weight loss is directly related to the overcharge developed by each charge strategy. Particularly, lower weight losses, of around 5 wt.% of the initial electrolyte weight, have been observed at 2.5 V cell^{-1} constant voltage, whereas due to the small overcharge generated by the boosting process, the cells maintain higher capacity during early cycles, but at the expense of a water loss increase, quantified as 11 wt.%

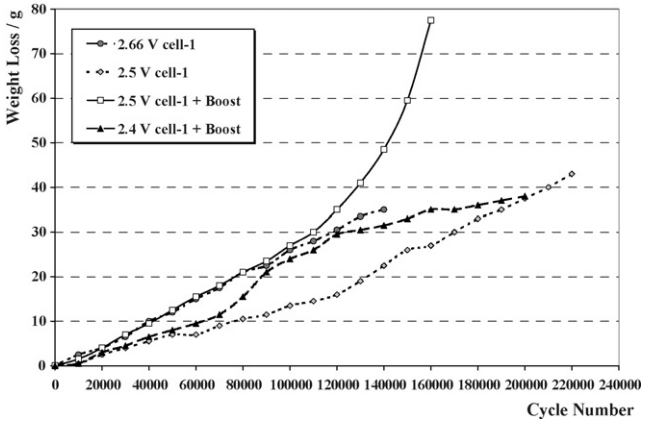

Fig. 13. Accumulated weight loss of modules with different charging profiles along the power assist cycle life test.

at failure after 160,000 cycles. Comparing the weight loss evolution of the different groups, constant voltage at 2.5 V cell^{-1} seems to be the best charge strategy among those tested, both from the practical point of view (boost would be very unreliable in the vehicles) and to extend life by reducing overcharging and the associated water loss and internal resistance increase due to corrosion phenomena.

3.5. Failure mode analysis

After reaching the failure criterion ($V < 1.5$ V cell^{-1}) in the different life tests, the modules were torn down for visual inspection and physical and chemical analyses of active materials, because PbO_2 and $PbSO_4$ contents and specific surface and porosimetry can provide valuable information about the different ageing mechanisms during cycling. Visual inspection showed mainly strong sulphation of the negative electrodes, specially in their upper part.

The analysis results of the different types of 6 V modules aged according to the power assist life test, in comparison to non-aged batteries, are shown in Table 4.

Samples of positive active material from aged batteries contain very high levels of lead dioxide (>95%), and show certain increase in the positive active material porosity, that indicates only moderate degradation, mostly in terms of specific surface area, that decreases with longer ageing periods. However, battery failure is clearly linked to irreversible sulphation of the negative active material, and mainly in the upper part of the electrodes (35–57% $PbSO_4$), as reported previously [5]. BET specific surface values are also lower in aged batteries and in the upper part of the electrodes, and are linked to lead sulphate levels and the number of cycles completed till battery failure.

Higher lead sulphate contents correspond to batteries charged at 2.66 V cell^{-1} and with lower saturation levels. Therefore, temperature increase associated to higher recombination rates and higher water loss seems to be a key factor on battery ageing and life duration.

3.6. Thermal study of a 36 V system

Temperature outside the modules in the positions defined previously in Fig. 1 was recorded by means of 6 thermocouples located in the 36 V battery, at the three different charging regimes and two cooling rates considered. Four thousand and two hundred cycles in total were recorded in each logging period, 700 for each charging and cooling conditions. Data showed clear differences between temperatures recorded by thermocouples B2 (lowest values, as it was located just over one of the fans) and A1 and A2 located on one battery side, which are clearly lower than those recorded by thermocouples B1, C2 and C1, the latter always with the highest values. As expected, the temperature difference was broader with the lower cooling rate.

The temperature values recorded by the different thermocouples along the test for the different cooling and charging rates led to conclude the following trends for the temperature evolution along ageing and at the different battery positions:

Table 4
Chemical composition, specific surface and porosity of negative and positive plates of 6 V VRLA batteries with different design and process conditions, aged according to power assist life test

Module batch and ageing conditions	Negative plates[a]		Positive plates			
	$PbSO_4$ (%)	BET ($m^2\ g^{-1}$)	PbO_2 (%)	$PbSO_4$ (%)	Porosity (%)	BET ($m^2\ g^{-1}$)
Non-aged modules	4.7	0.72	79.4	6.0	43.1	5.1
20 kPa 130,000 cycles	54.3 (T) 16.0 (B)	0.64 (T) 0.84 (B)	96.5	<0.2	53.1	1.24
45 kPa 130,000 cycles	52.5 (T) 39.3 (B)	0.62 (T) 0.72 (B)	96.5	<0.2	53.0	1.03
100 kPa 110,000 cycles	47.8 (T) 14.4 (B)	0.74 (T) 0.90 (B)	96.4	<0.2	54.2	1.41
90% 130,000 cycles	34.7 (T) 22.4 (B)	0.50 (T) 0.58 (B)	96.4	<0.2	52.8	1.69
95% 140,000 cycles	57.1 (T) 36.4 (B)	0.40 (T) 0.50 (B)	96.4	<0.2	54.6	1.35
100% 170,000 cycles	35.9 (T) 38.2 (B)	0.51 (T) 0.48 (B)	96.3	<0.2	53.0	1.10
2.4 V $cell^{-1}$ + boost 200,000 cycles	41.2 (T) 18.7 (B)	0.55 (T) 0.66 (B)	95.0	0.4	55.2	1.00
2.5 V $cell^{-1}$ 217,000 cycles	39.3 (T) 10.4 (B)	0.51 (T) 0.69 (B)	95.1	1.3	55.6	0.90
2.5 V $cell^{-1}$ + boost 163,000 cycles	41.6 (T) 22.3 (B)	0.46 (T) 0.59 (B)	95.7	1.1	53.2	1.41
2.66 V $cell^{-1}$ 140,000 cycles	57.1 (T) 36.4 (B)	0.40 (T) 0.50 (B)	96.4	<0.2	54.6	1.35

[a] T: top, upper part of the electrode; B: bottom, lower part of the electrode.

- Around 5 °C difference is observed between the highest (C1) and lowest (B2) temperatures recorded.
- Under similar charging and cooling conditions, only a small temperature increase is observed along life, just around 1 °C.
- For the same charging regime, 4–5 °C difference has been observed between high and low cooling rates.
- With the high cooling rate, temperature increase is just 1–2 °C when the charging voltage is increased, whereas for the low cooling rate, temperature increase is higher: 2–3 °C.

A calculation of the net overcharge, which is directly related to the charge acceptance, calculated for each 700 microcycle testing period, showed that charge acceptance is higher at higher voltage and lower cooling rates (higher temperature), as expected, and, for the different charging voltages, values at 45 V are more similar to 48 V than to those obtained at 43.2 V. Along ageing, a slight increase in net overcharge could also be appreciated.

In order to study the ageing degree in the different modules due to temperature gradients in the 36 V battery, the cycle life test was stopped after 64,200 cycles and then the modules were tested individually and their electrical performance compared to initial values, as shown in Table 5, in terms of capacity, internal resistance and weight loss for thermally equivalent modules 1–6, 2–5 and 3–4. The final capacity values were established after a charge/discharge/full charge conditioning cycle. Capacity and internal resistance values showed different ageing degrees for the different positions in the battery (external or internal) and the location of the fans under the modules. When compared with results of former tests, internal resistance and weight loss values correspond to an intermediate ageing degree.

After tear-down, the active materials from the modules referenced 1, 4 and 5 were analysed and results are included in Table 6, whereas Fig. 14 shows the SEM micrographs of the negative active material on the surface of the upper part of the negative electrodes. Analytical figures and photographs show an accumulation of lead sulphate mainly in the upper part of the negative electrodes, and the sulphate content is higher in module no. 5, in which the highest temperature values were recorded. Besides the increase of lead sulphate in the upper part

Table 5
Characterisation of modules before and after the thermal study

Modules no.	Weight loss (g)	R_i increase (%, 25 °C)	Capacity loss (%, first C_2)	Capacity loss (%, second C_2)	R_i increase (%, −18 °C)
1–6	24	17	31	23	45
2–5	36	23	39	25	56
3–4	26	17	34	27	47

Table 6
Chemical composition, specific surface and porosity of negative and positive plates of modules aged in different positions of a 36 V battery (64,200 power assist cycles)

Module no.	Negative plates[a]		Positive plates			
	$PbSO_4$ (%)	BET ($m^2\ g^{-1}$)	PbO_2 (%)	$PbSO_4$ (%)	Porosity (%)	BET ($m^2\ g^{-1}$)
Non-aged modules	4.7	0.72	79.4	6.0	43.1	5.1
1	15.5 (T) 11.8 (B)	0.75 (T) 0.78 (B)	95.8	<0.2	54.0	1.10
4	18.5 (T) 8.2 (B)	0.71 (T) 0.73 (B)	95.9	<0.2	51.7	0.91
5	36.6 (T) 13.4 (B)	0.70 (T) 0.71 (B)	96.0	<0.2	53.5	1.04

[a] T: Top, upper part of the electrode; B: Bottom, lower part of the electrode.

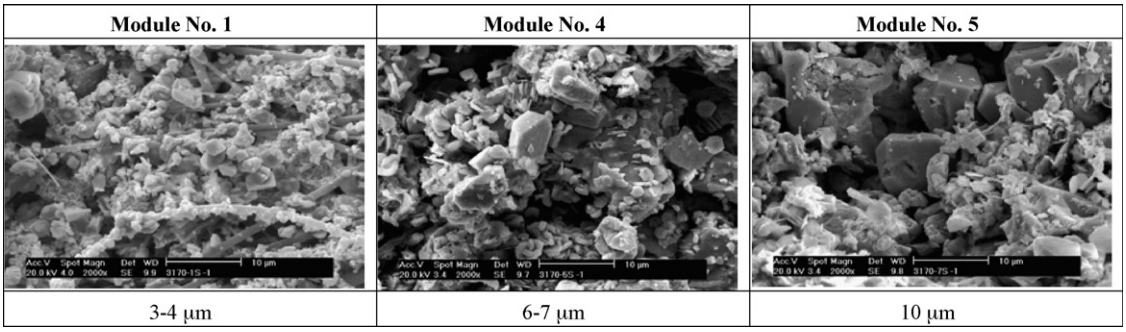

Fig. 14. SEM micrographs of negative active material from the surface of the upper part of negative electrodes of modules nos. 1, 4 and 5 of the 36 V battery after the thermal study.

of the negative electrode in the order module no. 1 < module no. 4 < module no. 5, the SEM micrographs of the surface of the upper part of the negative electrodes show that the crystal size also increased in the same order: the size of polyhedral lead sulphate crystals is 3–4 μm in module no. 1, 6–7 μm in module no. 4 and up to 10 μm in module no. 5. Photographs show also globular lead particles, equivalent to those observed in SEM micrographs of negative active material just after formation [5], especially when lead sulphate contents are low (i.e. modules nos. 1 and 4 in Fig. 14, or in the lower part of the electrodes).

4. Conclusions

In order to optimise life performance of spiral wound VRLA batteries under HRPSoC conditions, several design and process parameters (valve opening pressure and electrolyte saturation degree), as well as charging strategies, have been studied.

Valve opening pressure in operational range has a limited influence on cycle life results, and the best results have been obtained at intermediate pressure values (20–45 kPa), whereas a much higher pressure (100 kPa) seems to be unreliable, due to potential leakages in the polypropylene thermal welding area.

Excellent control of electrolyte saturation has been demonstrated and the exploitation of this characteristic in modules with high electrolyte saturation has led to an improvement in high rate partial state of charge cycle life of around 25% when comparing modules with initial 100% saturation degree with batches with 90–95% saturation degree.

According to the cycle life results, maintenance of available capacity appears to be improved with low constant voltage charging procedures (2.4–2.5 V $cell^{-1}$), whereas occasional boosting could be avoided by a consistent control of the state of charge of the modules. The cycle life results obtained (nearly 220,000 cycles at 2.5% DOD, and 60% SOC, that is equivalent to 5500 capacity turnover), confirm that the VRLA battery could be competitive for the claimed 10,000 capacity turnover of Ni–MH batteries.

A thermal study of a 36 V system, under a partial-state-of-charge-cycling test for hybrid electric vehicle applications has been carried out. Measurements of temperature in different locations of the battery when cycling the battery with different charging voltages and cooling rates has shown that the highest temperature difference between different locations in the battery is 5 °C, and a similar value is observed when comparing temperatures with high and low cooling rates. Battery ageing degree and charging voltage increase have a lower effect on temperature (1–2 °C increase).

Individual testing of modules located in different battery positions showed higher performance loss (in terms of available capacity and internal resistance increase) of modules with

higher working temperature along the test. Lead sulphate content in the upper part of the negative electrodes was higher in those modules, linked to larger lead sulphate crystals.

Acknowledgement

This project has been funded by the Advanced Lead Acid Battery Consortium (ALABC ISOLAB project).

References

[1] E. Karden, P. Shinn, P. Bostock, J. Cunningham, E. Schoultz, D. Kok, J. Power Sources 144 (2005) 505–512.
[2] F. Trinidad, C. Gimeno, J. Gutiérrez, R. Ruiz, J. Sáinz, J. Valenciano, J. Power Sources 116 (2003) 128–140.
[3] J. Valenciano, A. Sánchez, F. Trinidad, A. F. Hollenkamp, Proceedings of the LABAT 05 Conference, Varna, June 2005. J. Power Sources, 158 (2006) 851–863.
[4] Installation and Safety Optimised Lead Acid Battery for Mild Hybrid Applications (ISOLAB) Advanced Lead Acid Battery Consortium – Foresight Vehicle Project.
[5] M.L. Soria, J.C. Hernández, J. Valenciano, A. Sánchez, F. Trinidad, J. Power Sources 144 (2005) 473–485.
[6] EUCAR Traction Battery Working Group: Specification of Test Procedures for Hybrid Electric Vehicle Traction Batteries, September 1998.
[7] T. Ohmae, K. Sawai, M. Shiomi, S. Osumi, J. Power Sources 154 (2006) 523–529.
[8] R. Wagner in, D.A.J. Rand, P.T. Moseley, J. Garche, C.D. Parker (Eds.), Valve-regulated Lead-acid Batteries, Elsevier, Amsterdam, 2004, pp. 436–438.
[9] R.H. Newnham, in: D.A.J. Rand, P.T. Moseley, J. Garche, C.D. Parker (Eds.), Valve-regulated Lead-acid Batteries, Elsevier, Amsterdam, 2004, p. 479.